Calculation of Joule heating and temperature distribution generated in the KSTAR superconducting magnet structure

Seungyon Cho*, Jeong Woo Sa** and Chang Ho Choi*

Abstract: Since the KSTAR superconducting magnet structure should be maintained at a cryogenic temperature of about 4 K, even a small amount of heat might be a major cause of the temperature rise of the structure. The Joule heating by eddy currents induced in the magnet structure during the KSTAR operation was found to be a critical parameter for designing the cooling scheme of the magnet structure as well as defining the requirements of the refrigerator for the cryogenic system. Based on the Joule heating calculation, it was revealed that the bulk temperature rise of the magnet coil structure was less than 1 K. The local maximum temperature especially at the inboard leg of the TF coil structure increased as high as about 21 K for the plasma vertical disruption scenario. For the CS coil structure, the maximum temperature was obtained from the PF fast discharging scenario. This means that the vertical disruption and PF fast discharging scenarios are the major scenarios for the design of TF and CS coil structures, respectively. For the reference scenario, the location of maximum temperature spot changes according to the transient current variation of each PF coil.

Key Words: Joule heating, superconducting magnet structure, plasma disruption, current discharging

1. Introduction

The KSTAR superconducting magnet system producing the magnet field to confine and control the plasma during normal operation scenarios is composed of Toroidal Field (TF), Central Solenoid (CS) and Poloidal Field (PF) coil systems. The TF coils producing the magnetic field of 3.5 Tesla at the plasma center are normally under steady state operation. The PF and CS coils are, however, operated in pulse mode and produce the field variation as well as eddy currents in the magnet structure [1]. The TF and CS coil structures are composed of 16 and 8 identical segments, respectively. These segments are electrically insulated from each other to obstruct the eddy current induction in the structure during operation. Three operation scenarios are considered as the major concerning scenarios for the design of the superconducting magnet system. Plasma disruption is one of the major design-driving scenarios. It releases a significant amount of thermal energy in the magnet structure. A PF fast discharging scenario would be necessary if an abnormal condition happens in the PF coils or a quench occurs in the magnet system. Finally, during the reference operation, a relatively large current variation in the PF coils occurs. This produces eddy currents in the magnet structure, too. These operating scenarios are disclosed in Sec. 3, in more detail.

The Joule heating and its cumulative Joule energy by eddy currents affect the structural and thermal stability of the magnet system, because they might cause a very high local temperature rise in the cryogenic magnet structure. These would require an effective cooling scheme and burden the refrigerator of the cryogenic system.

In this paper, first the eddy currents induced in the magnet structure for three operation periods were calculated using the SPARK code [2]. Then Joule heating was estimated based on the eddy currents using a developed methodology [3]. Finally the temperature distribution in the magnet structure due to Joule heating was obtained using ANSYS [4], and the results were compared.

2. Description of Joule heating calculation model

In order to calculate the eddy current and Joule heating, a model was adopted, as shown in Fig. 1.

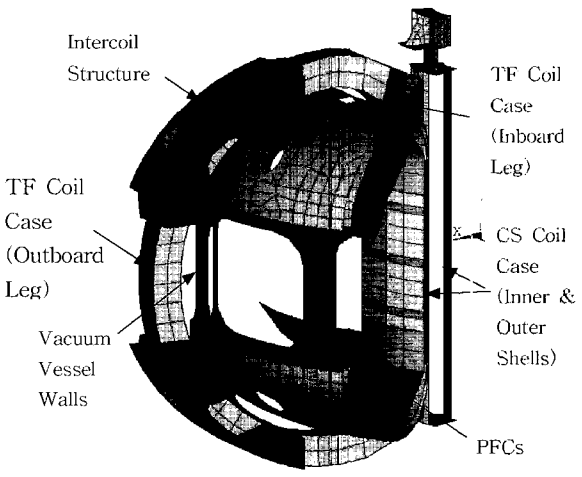

Fig. 1. A Joule heating calculation model

* 정 회 원 : 한국기초과학지원연구원 책임연구원
** 비 회 원 : 한국기초과학지원연구원 연구원
원고접수 : 2002년 03월 29일
심사완료 : 2002년 05월 07일

Table 1. Characteristics of the model for the joule heating calculation

Component		Electrical Resistivity (Ω-m)	Material	Thickness (mm)
PFCs	Limiter	7.8×10^{-7}	SUS316LN @300K	13.52/14/ 27.52
	Divertor	7.8×10^{-7}	SUS316LN @300K	17/21.25
	Passive Plate	2.13×10^{-8}	CuCrZrMg @300K	25
Vacuum Vessel Inner/Outer Wall		7.8×10^{-7}	SUS316LN @300K	10/12
TF Coil Structure		5.4×10^{-7} (no brazing) 5.303×10^{-7} (brazing)	SUS316LN @4K	58/48/67/ 32 58.2/48.2/ 67.2/32.2
CS Coil Structure		5.4×10^{-7}	SUS316LN @4K	80/48/12/ 117

This model includes plasma facing components (PFCs) without their support structures, inner and outer vacuum vessel walls without reinforcing ribs, one TF coil structure segment and one CS coil structure segment. A TF coil structure segment includes inboard and outboard legs for the coil case and a inter coil structure. An octant CS coil structure segment includes the support lug, flexible joint, top block, wedge, buffer and outer shell. The characteristics of the model are summarized in Table 1.

3. Operation scenarios

3.1. Plasma disruption scenario

There are two types of plasma disruption scenarios, radial and vertical disruptions. The vertical disruption is chosen because it produces more currents than radial disruption. So it adopted for the design of the superconducting magnet. Initial location of plasma is assumed such that the plasma has a major radius of 1.8 m, a minor radius of 0.5 m, and is positioned vertically in the mid-plane. The plasma moves upward about 60 cm over 120 ms. The relation between time and vertical position is Z (m) = 7.47-1x10-7 t(ms)3.8. During this period, the plasma also moves radially inward and its minor radius slightly decreases. After that, both a thermal and current quench occur over 5 ms and then the plasma disappears. These plasma movements during vertical disruption are shown in Fig. 2 [5].

3.2. PF coil current fast discharging

The current profiles for each PF coil during the PF fast discharging period are shown in Fig. 3. The currents almost disappear after 10 s. During this period no plasma is expected, so the plasma current is not considered here. The current in the TF coil still exists and considered here.

3.3. Reference scenario

The reference scenario consists of initial magnetization (IM), blip, start of flattop (SOF), start of burn (SOB), end of burn (EOB), and end of current (EOC) as shown in Fig. 4. The plasma current starts at 0 s and reaches 2 MA at 4.26 s.

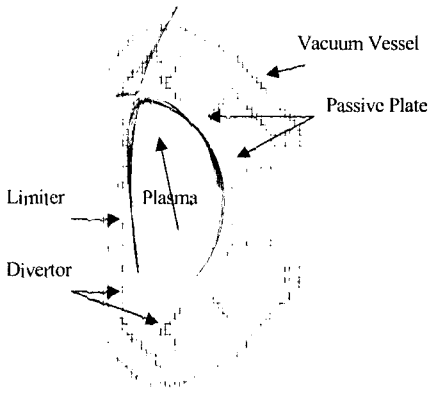

Fig. 2. Plasma movement during vertical disruption

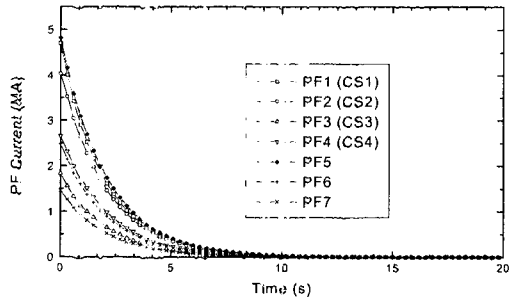

Fig. 3. PF currents during PF fast discharging

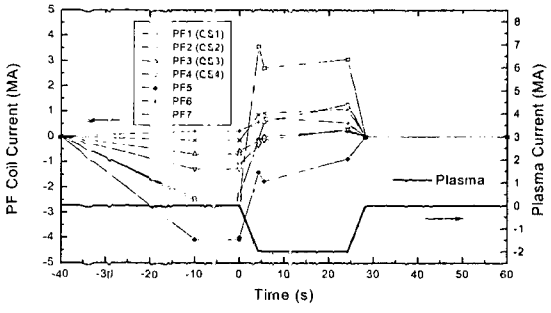

Fig. 4. PF coil currents and plasma current in reference scenario: PF-on at -40 s; Initial Magnetization (IM) at -10 s; Blip-on at 0 s; Blip-off at 0.06 s; Start of Flattop (SOF) at 4.26 s; Start of Burn (SOB) at 5.56 s; End of Burn (EOB) at 24.26 s; and End of Current (EOC) at 28.26 s.

The plasma current starts to decrease at EOB and disappears completely at EOC. The current profiles in the PF coils show that significant current variations occur during the blip, SOF and EOC periods [1].

4. Calculation of Joule heating

Eddy currents generated in the magnet structure were obtained using SPARK code for the defined operation scenarios. One of representative eddy current distribution on the TF magnet structure is shown in Fig. 5 for the plasma disruption scenario at 200 ms. The currents are concentrated on the upper part of the inboard leg, where large joule heating is expected. Transient Joule heating was calculated based on the eddy currents. The Joule heating in the TF and CS coil structures during a plasma vertical disruption has maximum at 125 ms and 126 ms, respectively. The cumulative Joule energy at 200 ms for the TF and CS coil structure segments are 20.3 kJ and 1.2 kJ, respectively. The profile of the Joule heating and the transient cumulative Joule energy generated in the TF and CS coil structure segment are shown in Fig. 6.

The Joule heating in the magnet structure during the PF fast discharging period has maximum at 0.3 s. The profiles of the maximum Joule heating and the transient cumulative Joule energy generated in the TF and CS coil structure segments are shown in Fig. 7. Once the Joule heating reaches the maximum value at 0.3 s, it decays exponentially and then almost disappears at 9 s. The cumulative Joule energy in the TF coil structure for the PF fast discharging scenario is about 65 percent of that for the disruption case. However, the energy in the CS coil structure for the PF dump scenario is about 2.72 kJ, that is twice that for the disruption case. Therefore, it can be mentioned that the effect of Joule heating on the CS coil structure is more dominant in the PF fast discharging scenario than in the disruption case.

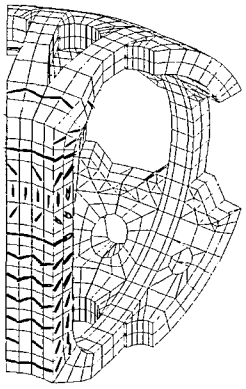

Fig. 5. Eddy current distribution generated on the magnet structure for the plasma vertical disruption scenario

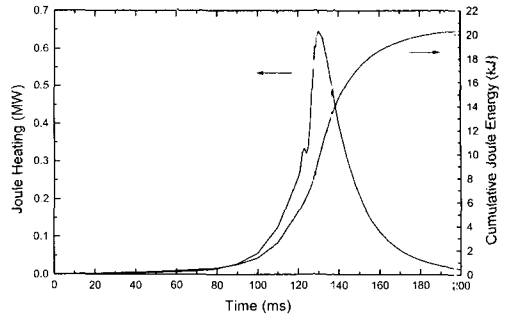

(a) TF coil structure segment

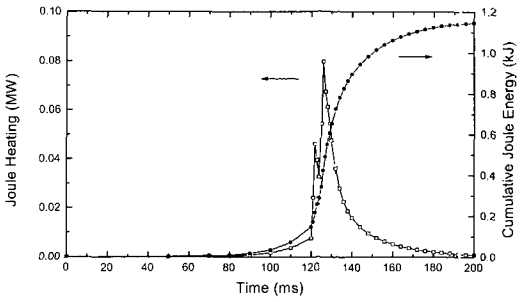

(b) CS coil structure segment

Fig. 6. Transient Joule heating and cumulative Joule energy during a vertical disruption

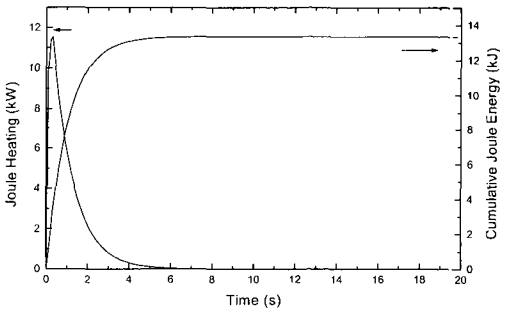

(a) TF coil structure segment

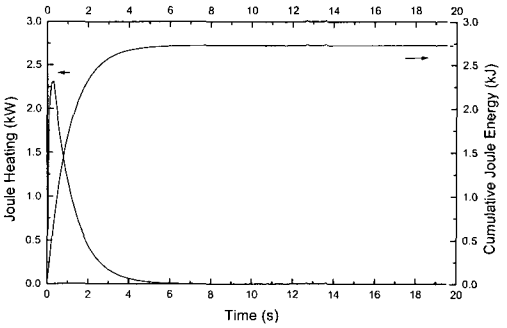

(b) CS coil structure segment

Fig. 7. Transient Joule heating and cumulative Joule energy during PF fast discharging scenario

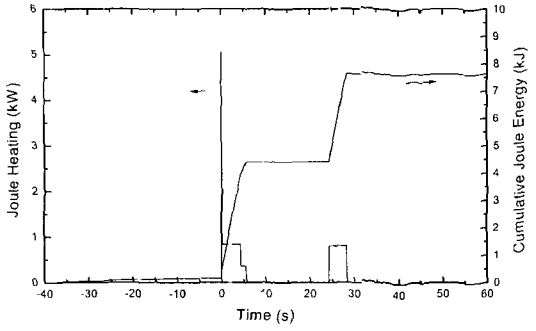

(a) TF coil structure segment

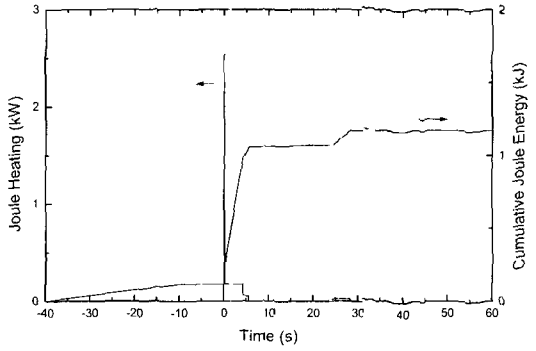

(b) CS coil structure segment

Fig. 8. Transient Joule heating and cumulative Joule energy in the reference scenario

The Joule heating generated in the magnet structure for the reference scenario has maximum during blip period of 0.06 s. The transient profile of the Joule heating and the cumulative Joule energy of the TF and CS coil structure segments are shown in Fig. 8. During the blip period the current increase rate in PF coils is up to 3 MA/s. In the successive period up to SOF, the relatively steep increase rate of currents in PF coils results in large eddy currents and therefore relatively large Joule heating is generated. The next large current jump period is between EOB and EOC. Here the third largest peak of Joule heating is generated. At these peaks the cumulative Joule energy has large jumps as also shown in Fig. 8. Since the Joule heating generated in the magnet structure reaches the steady state quickly if there are no current variations in each coil, a flat curve can be easily found in the cumulative Joule energy profile. The Joule heating disappears completely after 28.46 s for the TF and 28.36 s for the CS coil structures, respectively.

5. Calculation of temperature distribution

Based on the transient Joule heating and cumulative Joule energy profiles shown in Figs. 6 through 8, the transient temperature distribution on the TF and CS coil structures was obtained using ANSYS. The maximum temperature distribution was also obtained at 200 ms, 9 s, and 60 s for the vertical disruption, PF fast discharging, and reference scenario, respectively, as shown in Figs. 9 through 11. For the vertical disruption scenario, the maximum temperature was created in the inner wall of inboard leg of the TF coil structure. This relates to the current distribution as shown in Fig.5, where the currents were circulating in the upper part of the inboard leg. The temperature in the side and outer walls of the inboard leg is much lower. Since the plasma moves upward, the maximum Joule heating was generated in the upper local area of the inboard leg where the maximum temperature was up to 20.6 K. The temperature in the outboard leg was barely changed from the bulk temperature of 4 K.

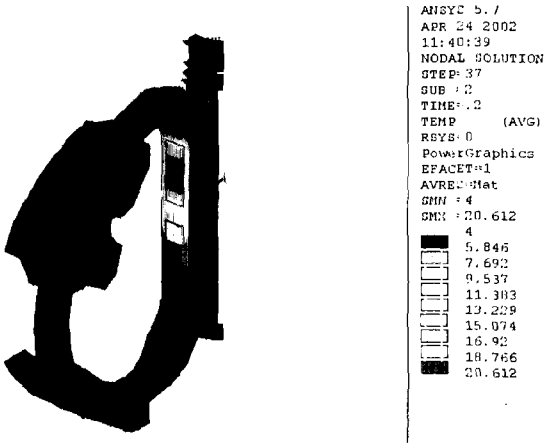

Fig. 9. Temperature distribution based on the cumulative Joule energy at 200 ms during the vertical disruption scenario.

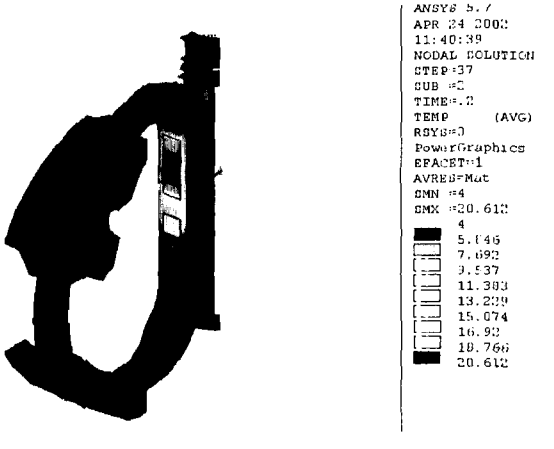

Fig. 10. Temperature distribution based on the cumulative Joule energy at 9 s during the PF fast discharging scenario.

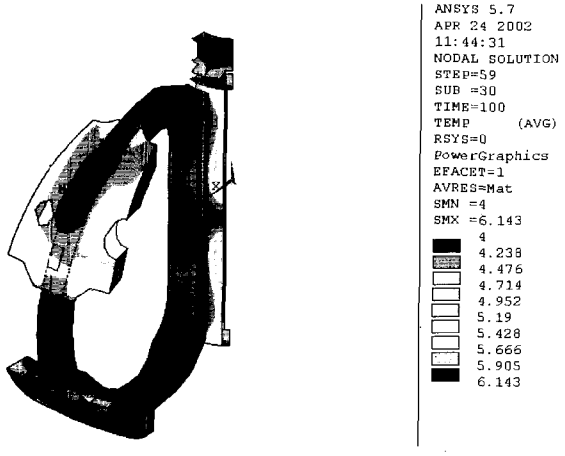

Fig. 11. Temperature distribution based on the cumulative Joule energy at 60 s during the reference scenario.

During the PF fast discharging period, the eddy currents were concentrated on the interface between the TF coil case and the inter-coil structure, as well as at the upper part of the CS coil structure. The maximum temperatures in the TF and CS coil structures increased up to 9.5 K and 8.4 K, respectively. For the reference scenario the maximum temperature was generated in the port hole of the TF inter-coil structure and the middle part of the CS coil structure. This temperature is much lower than the results of the previous two operation scenarios. But the location of the maximum temperature zone is different for all three scenarios.

The transient temperature histories at the maximum temperature point for three operation scenarios are shown in Figs. 12 through 14. The temperature history seems to follow the cumulative Joule energy profile shown in Figs. 6 through 8. But for the reference scenario, during the blip period the maximum temperature was found at the top/bottom sections of the CS outer shell. Also, over the whole period up to EOB the temperature at the middle section of the CS outer shell is maximum. After EOC large Joule heat is generated in the TF coil structure due to plasma current variation, so the temperature in the TF coil structure becomes maximum.

The bulk temperature rise of the CS and TF coil structure segments was also calculated based on the cumulative Joule energy in order to investigate the inherent temperature variation due to joule heating. It was found that the bulk temperature increase is no more than 1 K for both segments during the periods of the operation scenarios. Although the bulk temperature is negligibly small, if abnormal events occur successively before the magnet structure is completely cooled down the energy will be added up and result in a higher bulk temperature. The time interval between the abnormal events can serve as a criterion for the operation scenario. The above mentioned all results were summarized in Table 2.

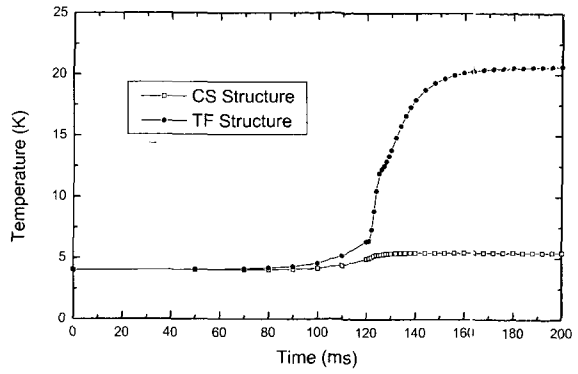

Fig. 12. Temperature history at the maximum temperature points during a vertical disruption

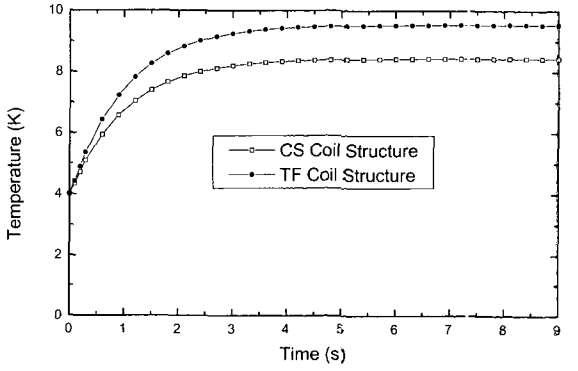

Fig. 13. Temperature history at the maximum temperature points during PF fast discharging

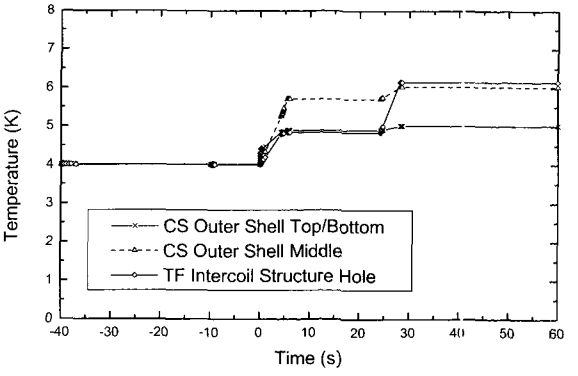

Fig. 14. Temperature history at the maximum temperature points for the reference scenario

Table 2. Summary of maximum Joule heating, cumulative Joule energy, maximum temperature and bulk temperature increase

Operation Scenario	Plasma Vertical Disruption		PF Fast Discharging		Reference	
Coil Type	TF	CS	TF	CS	TF	CS
Max. Joule Heating, [kW]	646	80	11.6	2.3	5.1	2.5
Cumulative Joule Energy, [kJ]	20.3	1.2	13.3	2.73	7.6	1.2
Maximum Temperature, [K]	20.6	5.4	9.5	8.4	6.1	6.0
Bulk Temperature rise, [K]	0.93	0.46	0.61	1.04	0.35	0.46

6. Conclusion

The Joule heating and the cumulative Joule energy generated in the TF and CS coil structures during vertical disruption, PF fast discharging, and reference scenario were calculated. The overall temperature distribution in the TF and CS coil structures was estimated based on the Joule heating. A local maximum temperature zone was generated in the inboard leg of TF coil structure. The maximum temperature in the CS coil structure was important in the PF fast discharging case rather than in the disruption case. However although the bulk temperature is negligibly small, the localized temperature can be cooled down by the magnet structure cooling scheme. In conclusion, the magnet structure were safely designed with regrads to the operating scenarios.

Acknowledgement

This work was supported by the Ministry of Science and Technology the Republic of Korea under the KSTAR Project Contract.

References

[1] C.H. Choi, et al., "Electro-magnetic loads on the KSTAR magnet system", 17th international conference on Magnet Technology (MT-17), Sep. 24-28, Geneva, Switzerland, 2001. Also, IEEE Trans. Applied Superconductivity submitted for publication.

[2] D.W. Weissenburger, "SPARK version 1.1 User Manual", Princeton Plasma Physics Laboratory, Report No. PPPL-2494, 1988.

[3] S. Cho and J.W. Sa, "Benchmark test for the eddy current and Joule heating calculation with ANSYS-EMAG and SPARK codes', Korea Basic Science Institute, Memorandum No. 141 & 149, Feb. 2000.

[4] ANSYS, Inc., 201 Johnson Road, Houston, PA 15342, USA.

[5] S. Cho, et al., "Design analysis of electromagnetic forces on the KSTAR vacuum vessel interfaces", Fusion Engineering and Design 51-52, pp. 219-227, 2000.

저 자 소 개

조승연(趙昇衍)
1961년 8월 2일생, 1984년 한양대 공대 기계공학과 졸업, 1986년 한국과학기술원 기계공학과 졸업 (공학석사), 1994년 UCLA 기계항공원자력학과 졸업 (공학박사), 현재 한국기초과학지원연구원 책임연구원

사정우(史政祐)
1971년 11월 7일생, 1997년 충남대 의교 기계설계공학과 졸업, 1999년 동 대학원 기계설계공학과 졸업(공학석사), 현재 한국기초과학지원연구원 연구원.

최창호(崔昌鎬)
1963년 3월 5일생, 1988년 경북대 자연대 물리학과 졸업, 1990년 동 대학원 물리학과 졸업(이학석사), 1995년 동 대학원 물리학과 졸업(이학박사), 현재 한국기초과학지원연구원 책임연구원